Variability of satellite-derived sea surface height anomaly, and its relationship with Bigeye tuna (Thunnus obesus) catch in the Eastern Indian Ocean

Jonson Lumban-Gaol, Robert R. Leben, Stefano Vignudelli, Kedarnath Mahapatra, Yoshihiro Okada, Bisman Nababan, Marisa Mei-Ling, Khairul Amri, Risti Endriani Arhatin & Muhammad Syahdan

Submit your article to this journal ⤢

View related articles ⤢

View Crossmark data ⤢

Variability of satellite-derived sea surface height anomaly, and its relationship with Bigeye tuna (*Thunnus obesus*) catch in the Eastern Indian Ocean

Jonson Lumban-Gaol[1]*, Robert R. Leben[2], Stefano Vignudelli[3], Kedarnath Mahapatra[4], Yoshihiro Okada[4], Bisman Nababan[1], Marisa Mei-Ling[5], Khairul Amri[6], Risti Endriani Arhatin[1] and Muhammad Syahdan[7]

[1]Department of Marine Science and Technology, Bogor Agricultural University, Bogor 16680, Indonesia
[2]University of Colorado, Boulder, CO 80309-0431, Colorado, USA
[3]Consiglio Nazionale delle Ricerche (CNR), Via G. Moruzzi, 1 Pisa, Italy
[4]School of Marine Science and Technology, Tokai University, 3-20-1 Orido, Shimizu, 424-8610, Japan
[5]Center for Geomatics Engineering (CGE), Surya University, Serpong, Tangerang, Indonesia
[6]Ministry of Fisheries and Marine Affairs, Jakarta, Indonesia
[7]Faculty of Fisheries and Marine Sciences, Lambung Mangkurat University, Banjar Baru 70721, Indonesia
*Corresponding author, e-mail address: jonson_lumbangaol@yahoo.com

Abstract
We analyzed the variability of sea surface height anomaly (SSHA), and its relationship with Bigeye tuna catch in the eastern Indian Ocean (EIO) off of Java Island (Indonesia). Both time series of SSHA and Bigeye tuna HR show dominant signals corresponding to the annual and inter-annual variability. During the southeast monsoon the wind blows along southern coast of Java and produces coastal upwelling. This causes sea level to drop due to an offshore Ekman transport, and thermocline becomes shallower. During El Niño and Indian Ocean Dipole (IOD) positive phase, upwelling is more intense and a large cold eddy forms in the EIO off Java. Generally, Bigeye tuna HR tends to increase during upwelling seasons and becomes even higher during El Niño and the positive phase of the IOD. The increased Bigeye tuna HR during the southeast monsoon, El Niño and the IOD positive phase can be attributed to the shallower thermocline depth and the enhancement of biological productivity due to development of eddies and strong upwelling in the EIO. The spatial distribution of SSHA indicates that Bigeye tuna catches are abundant in the frontal regions between cold and warm eddies.
Keywords: Bigeye tuna, eddy, El Niño, satellite radar altimetry, sea surface high anomaly.

Introduction
The eastern Indian Ocean region off Java Island (04ºS-16ºS and 105ºE-120ºE) has long been considered important for the Indonesian Bigeye tuna fishing industry. Since 1992 the Indonesian government has operated a fleet of 20 longline tuna fishing boats in the EIO region, consisting of 9 ships of 100 Gross tonage (GT) and 11 ships of less than 100 GT. The dominant catch in EIO region was Bigeye tuna (73%) with the remainder (23%)

consisting of Yellowfin tuna, marlin and shark. The productive pelagic fisheries in this area are sustained through enhanced biological productivity due to seasonal coastal upwelling during the southeast monsoon [Wyrtki, 1962; Susanto et al., 2001]. The EIO region is also affected by Indonesian Throughflow (ITF), the transport of Pacific Ocean water to the Indian Ocean through the Indonesian seas [Godfrey, 1996]. Moreover, Susanto et al. [2001] stated that the interannual variability of the upwelling in the EIO region is linked to El Niño Southern Oscillation (ENSO) through the ITF, and also is influenced by the IOD as well [Saji et al., 1999; Feng and Meyers, 2003].

There is good evidence that ENSO events have an impact on the recruitment of tuna, their distribution, composition, and species abundances [Lehodey et al., 1997; Lumban-Gaol et al., 2002; White et al., 2004]. Měnard et al. [2007] reported strong associations between tuna catch and 4- and 5-yr periodic modes in climate time series, namely the periodic band of El Niño signal propagation in the Indian Ocean. El Niño and IOD events are associated with physical and biological changes in the oceans such as SST, wind speed, current movements, depth of mixing layer, eddies upwelling period and intensity [Rasmusson et al., 1982; Susanto et al., 2001]. During the El Niño coinciding with the IOD positive phase 1997/98, anomalous easterly winds induced strong upwelling along the southern coasts of Java and Sumatra. This event produced higher phytoplankton concentrations [Susanto and Mara, 2005]. Phytoplankton are eaten by herbivores called zooplankton. In turn, zooplankton provide food for krill and some small fish. The timing of phytoplankton blooms plays a large role in maintaining marine ecosystems, and is therefore crucial to the survival of fish.

Syamsuddin et al. [2013] stated that the 1997/98 ENSO significantly affected the oceanographic conditions that influence Bigeye tuna catchability and concluded that SST is a good predictor of Bigeye tuna fishing grounds in the EIO region. However, according to Mohri et al. [1996], Bigeye tuna distribution is better predicted by thermocline parameters, rather than by SST directly. Their study revealed that Bigeye tuna prefer to stay near, and usually below the thermocline. The results of several studies showed that the optimum water temperature at hook depths for Bigeye tuna ranges between isotherm $10°$-$15°C$ ($IT_{10°-15°}$), which is below the thermocline depth [Mohri et al., 1996; Hanamoto, 1987]. Based on these studies we assumed that it is difficult to use SST as a predictor for Bigeye tuna fishing ground in the EIO region. Therefore, we support the idea that SSHA could a good indicator to predict Bigeye tuna fishing grounds because of the relationship between sea level variations and thermocline depth [Bray et al., 1996]. Susanto et al. [2001] found a significant correlation between thermocline depth and sea level in EIO region. During El Niño, the thermocline depth was about 20 to 60 m shallower than observed in normal climate condition [Susanto et al., 2001]. In the Bengal Bay, the evolution of SSHA and the depth of $20°C$ (D_{20}) isotherm indicated that the temporal variability of the two quantities was similar with low sea surface height (negative values) corresponding to negative anomaly (shallow) D_{20} [Yu, 2003]. Therefore, SSHA can be used as a proxy thermocline depth indicator.

Data and methods

SSHA data were produced by the Colorado Center for Astrodynamics Research (CCAR) at the University of Colorado. The SSHA is generated by subtracting the temporal mean SSH time series from the original data set. Details about SSHA data processing and analysis can be found in Leben et al. [2002]. SSHA data from 1994 to 2007 were utilized for this study,

whereas Chl-a concentrations were from 1998 to 2007 derived from Sea-viewing Wide Field-of-View Sensor (SeaWiFS) and MODerate resolution Imaging Spectro-radiometer (MODIS) [Tucker and Yager, 2011]. The reasons for the use of data over different time periods is because tandem sampling from TOPEX/Poseidon and ERS-1 satellite altimeters began in October 1992, while ocean color derived from SeaWiFS was available only since August 1997. The meridional section of temperature was derived from buoy measurements deployed in the EIO region by the Geophysical Fluid Dynamic Laboratory (GFDL), National Oceanic and Atmospheric Administration (NOAA) and eXpendable Bathy Thermograph (XBT) measurements from the World Ocean Database 2005 (WOD-2005). The Chl-a concentrations, SST and wind data were obtained from Giovanni-Interactive Visualization and Analysis [Acker and Leptoukh, 2007] and NOAA CoastWatch. Ocean Data View software was used to process the vertical distribution of temperature derived from buoys and XBT measurements.

Bigeye tuna catch datasets were collected from several different sources, including: (1) daily tuna catches obtained from 14,000 settings of longlines under 20 tuna longliners boats operated in the EIO region, and (2) monthly average HR derived from reports (1992-2005) by the tuna fishing company "PT. Samoedra Besar" in Bali, Indonesia. Bigeye tuna HR was calculated from the total of bigeye tuna caught in 100 hooks of longline. The catch rates were computed and the spatial distribution of Bigeye tuna HR plotted in the EIO region. The study area and the spatial distribution of Bigeye tuna HR are shown in Figure 1.

Time series analysis was carried out to understand the variability of both SSHA and Bigeye tuna HR. Statistical cross-correlation analysis was carried out to evaluate the strength of time-lagged relationship between ENSO/IOD and SSHA as well as SSHA and HR which are represented by the following equations:

$$r_{xy}(k) = \frac{C_{xy}(k)}{S_x S_y} \quad [1]$$

where,

$$C_{xy}(k) = \begin{cases} \sum_{t=1}^{n=k} (x_t - \bar{x})(y_{t+k} - \bar{y}), k = 0,1,2,...,(n-1) \\ \sum_{t=1-k}^{n} (x_t - \bar{x})(x_{t-k} - \bar{y}), k = -1,-2,...,-(n-1) \end{cases} \quad [2]$$

$$S_x = \sqrt{\frac{1}{n}\sum_{t=1}^{n}(x_t - \bar{x})^2} \quad [3]$$

$$S_y = \sqrt{\frac{1}{n}\sum_{t=1}^{n}(y_t - \overline{y})^2} \quad [4]$$

and x_t: SSHA or HR series of length n, y_t: SOI/DMI indices series of length n, $\overline{x}, \overline{y}$: sample means, $r_{xy}(k)$: sample cross correlation coefficient at lag k, S_x: standard deviation of series x, S_y: standard deviation of series y, $C_{xy}(k)$: sample cross covariance at lag k.

The Continuous Wavelet Transform (CWT) was used to analyze the signal in the SSHA and HR time series data, which produces an instantaneous estimate or local value for the amplitude and phase of each harmonic. The CWT of the non-stationary spatial or time dependent signal characteristics is given by Torrence and Compo [1998] as:

$$W_n(s) = \sum_{n=0}^{N-1} x_n \cdot \psi * \left[\frac{(n'-n)\delta t}{s}\right] \quad [5]$$

where x_n is a time series with equal time spacing δt and $n=0...N-1$ and ψ is a wavelet function, that depend on non-dimentional 'time'. The (*) indicates the complex conjugate. The wavelet transform can be used as a band-pass filter of uniform shape and width, as described in detail in Torrence and Compo [1998]. Here, the low-frequency band-pass filter of SSHA and HR time series is used to extract the annual and interannual signals.
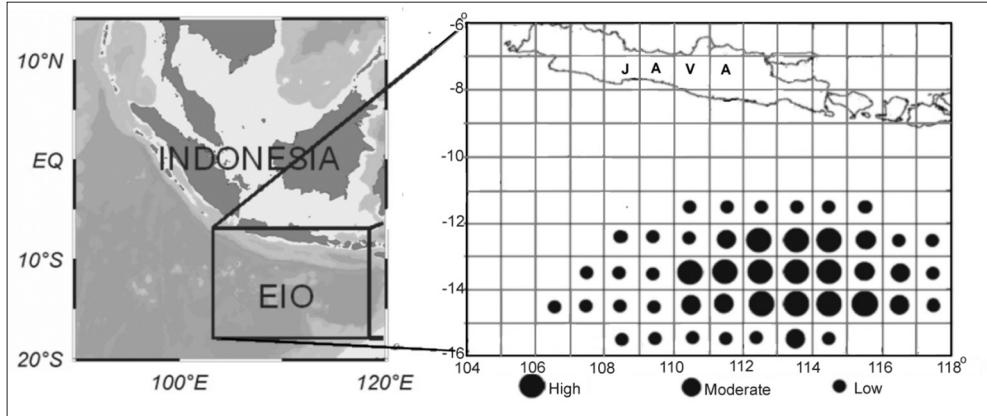

Figure 1 - EIO region (area of investigation) and spatial distribution of monthly average Bigeye tuna HR derived from statistics reports (1994-2005). The big, medium, and small circles show the area with high, moderate, and low frequency of tuna HR > 0.8.

Results and discussions
Long term data
The monthly mean time series of the SOI and DMI indices, SSHA, thermocline depth, Chl-a concentrations, and Bigeye tuna HR are shown in Figure 2. SSHA shows a seasonal pattern, i.e., negative (<-10 cm) during southeast monsoon when upwelling occurs (June-October) and conditions are reversed to positive (>10 cm) during northeast monsoon when

downwelling occurs (December-April) (Fig. 2b). The decrease of sea surface height during upwelling, has resulted in thermocline shallowing (Fig. 2c) and caused a corresponding shallow Bigeye tuna fishing layer of at least 50 m depth. The shallow depth enables the longliners to penetrate deeper into the Bigeye tuna fishing layer and is one of the causal factors that increase tuna hook rate during southeast monsoon season (Fig. 2d).
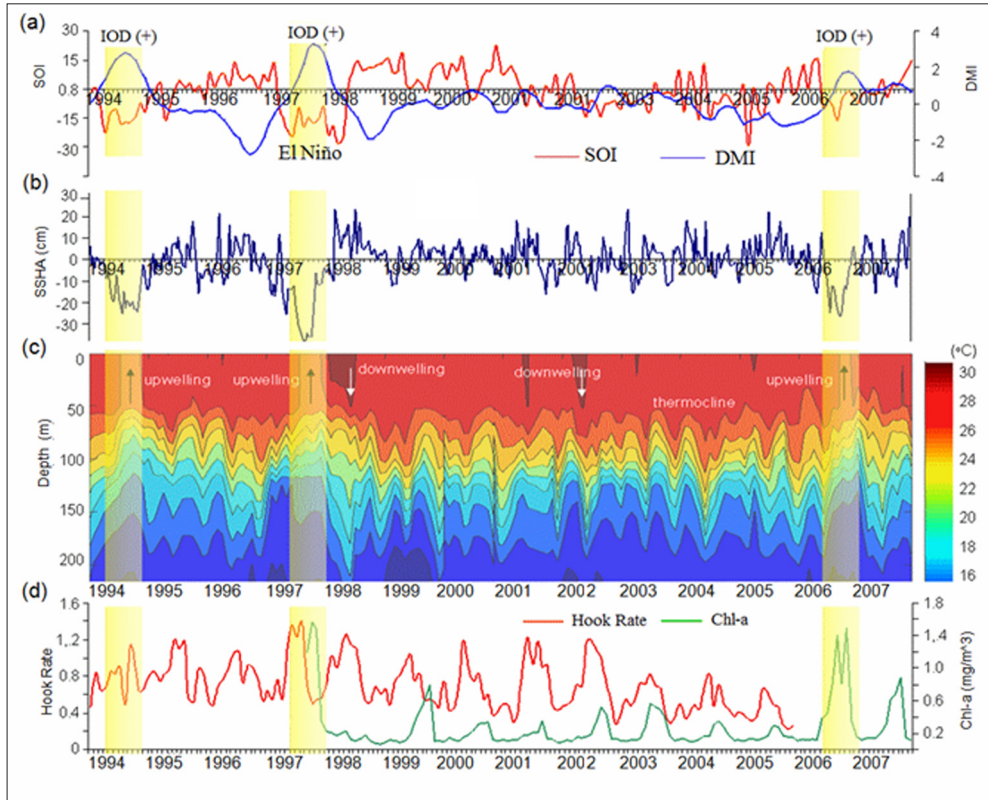

Figure 2 - Time series of Southern Oscillation Index and Dipole Mode Index (a), SSHA (b), thermocline layer depth (c) and Chl-a concentrations and Bigeye tuna HR (d).

Chlorophyll-a concentrations can also be used as a valuable indicator to identify seasonal variations, i.e. the relatively high concentrations (>0.3 mg/m^3) during the southeast monsoon and relatively low concentrations (<0.1 mg/m^3) during the northeast monsoon (Fig. 2d) except in 1999 and 2002 during La Nina conditions. Southeasterly wind from Australia during the southeast monsoon generates upwelling (Fig. 3b), and increases nutrients at the surface along the southern coasts of Java and Sumatra [Susanto and Mara, 2005]. Phytoplankton blooms during the upwelling events becomes a source of food for small fish, which in turn are a food source for top predators. This causes the hook rate for Bigeye tuna to be high during this time period (Fig. 2d).

In general, during the southeast monsoon upwelling manifests lower SST and lower SSH but higher chl-a concentration (Fig. 3). During the 1997/1998 El Niño, which coincided

with the IOD positive phase [Susanto et al., 2006; Meyer et al., 2007], and during the 2006/07 IOD the upwelling associated with the southeast monsoon was intensified. Hence both the 1997/98 El Niño (and IOD) and the 2006/07 IOD positive phase further enhanced the highest chlorophyll-a concentration and lowest SST in the EIO region (Fig. 3).
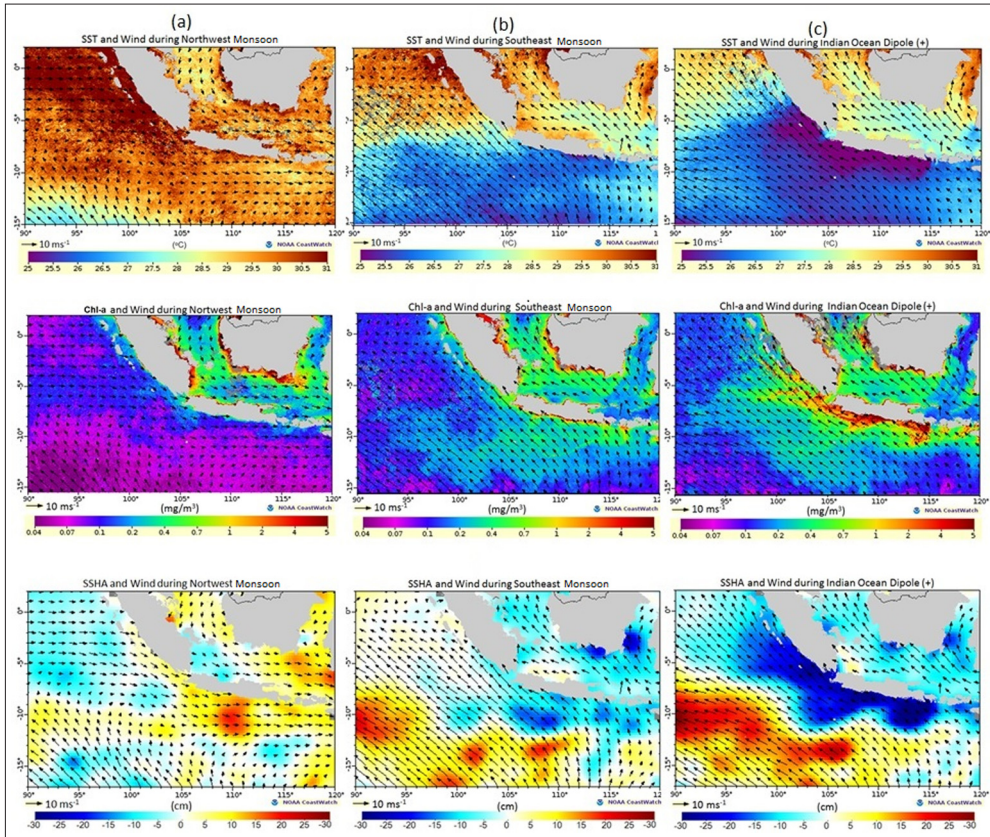
Figure 3 - (a) The SST, Chl-a and SSHA during northwest monsoon, (b) during southeast monsoon (upwelling) and (c) Indian ocean El Niño and IOD positive phase (intensified upwelling).

In the EIO region, the evolution of SSHA and the depth of $IT_{10^\circ\text{-}15^\circ}$ indicates that the temporal variability of the two quantities were similar with negative SSHA corresponding to shallow $IT_{10^\circ\text{-}15^\circ}$. Our results are consistent with previous studies that reported that sea surface height correlates with thermocline depth in the Indian Ocean and Bengal Bay [Bray et al., 1996; Yu, 2003].

Horizontal and vertical movements of various tuna are influenced by oceanographic conditions. The predominant Bigeye tuna daytime distribution was between 220 and 240 m due to suitable temperature for their distribution [Holland et al., 1990]. Temperature and thermocline depth seemed to be the main environmental factors governing the vertical and horizontal distribution of Bigeye tuna. The optimum temperature of Bigeye tuna for fishing is $IT_{10^\circ\text{-}15^\circ}$ [Hanamoto, 1987]. The depth of $IT_{10^\circ\text{-}15^\circ}$ in the EIO region varies from 150 to 400 m, whereas the tuna longline is normally set to reach water depths of only 100 to 280 m.

During El Niño and the IOD positive phase the $IT_{10°-15°}$ depth, which associated with the fishing layer for Bigeye tuna, is 40-60 m shallower than normal conditions [Susanto et al., 2001]. This reflects an increase of Bigeye tuna HR during El Niño since the fishing layer is shallower than normal, therefore resulting in a growing number of hooks reaching the Bigeye tuna fishing layer.

Time series data for HR of Bigeye tuna over 10 years showed that during the upwelling period the Bigeye tuna HR generally increase (>0.6) and is higher during El Niño and IOD positive phase (> 0.8) except in 1994 (Fig. 2d). Although Bigeye tuna HR of fishing vessels from the fisheries company "PT. Samoedra Besar" which operated in EIO region off Java was low in 1994, the total fish landing in the EIO region off Sumatra is higher than normal [Amri, 2012]. This may indicate that the abundance of Bigeye tuna was high, but the catchability of the tuna with longlines was low.

The overall trend of Bigeye tuna HR during 1994-2005 showed a negative linear trend. Based on data published by the Indian Ocean Tuna Commission (IOTC), the Bigeye tuna production in the EIO region from 1994 to 2007 also saw a significant decrease (Fig. 4) [Lumban-Gaol et al., 2012]. Tuna fish stock has declined in the EIO region and the decline is likely caused by over fishing [Saputra et al., 2011].
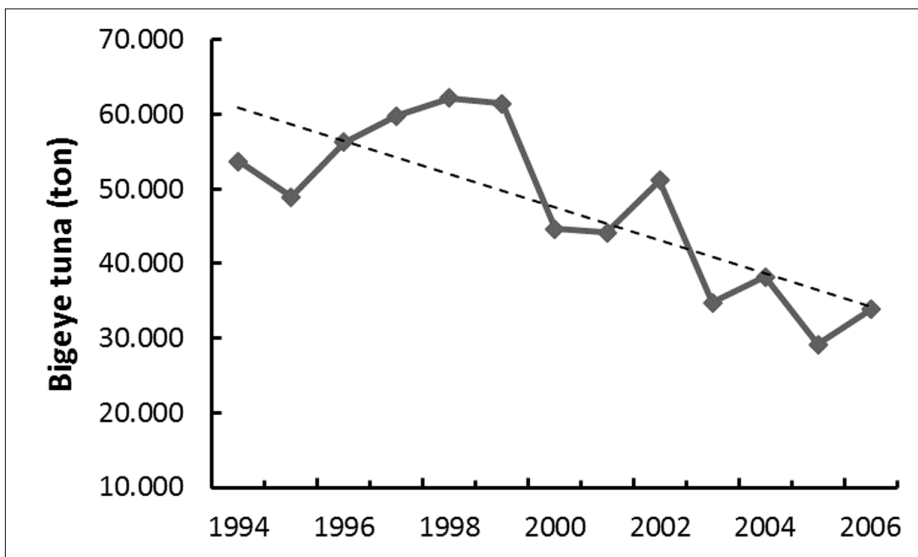

Figure 4 - Trend of Bigeye tuna catch in Eastern Indian Ocean (1994-2006) (www.iotc.org).

Figure 5 shows the time series of the wavelet coefficient for the annual and interannual signals in both SSHA and Bigeye tuna HR. The SSHA variability on annual time scales clearly shows that the SSHA is negative during the southeast monsoon (July-September) and is positive during the northwest monsoon (December-February) in the EIO region. The highest amplitude of SSHA occured in 1997-1999 during the El Niño/IOD and La Niña. The Bigeye tuna HR variability on annual time scales exhibits a maximum during the southeast monsoon and a minimum during the northwest monsoon. The response of the Bigeye tuna HR is clearly seen during the 1997/98 and 2002/03 El Niño events (Fig. 5d).
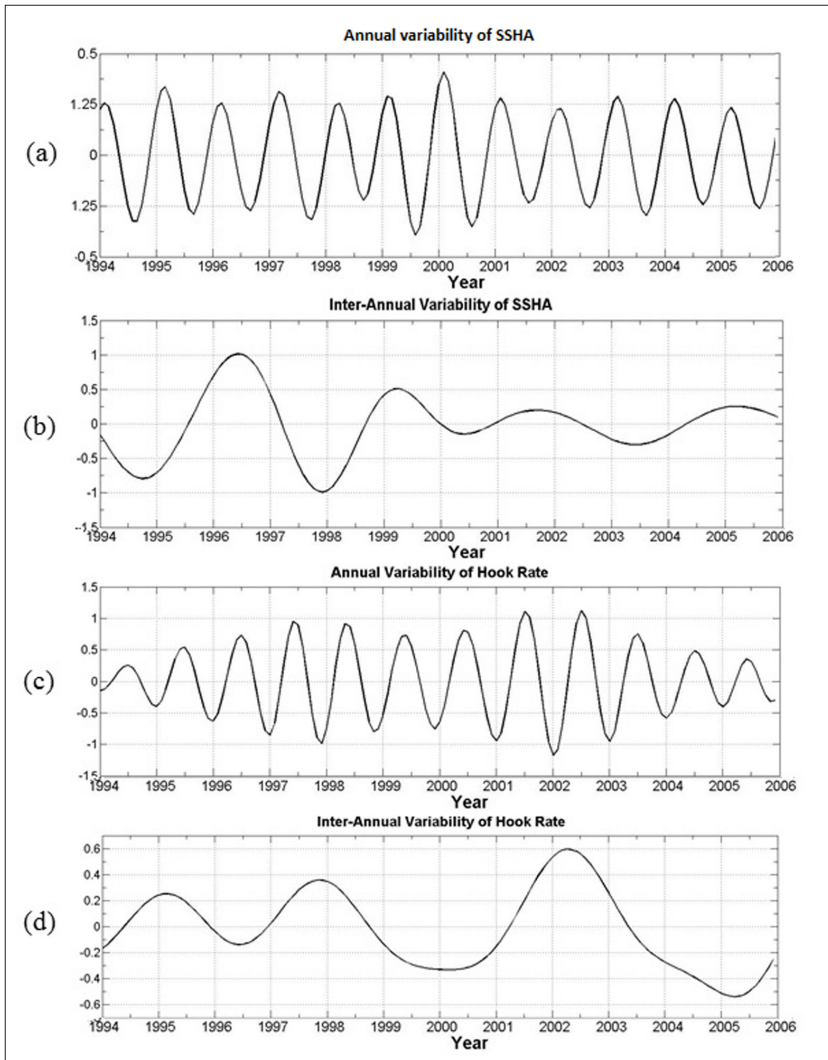
Figure 5 - Time variations of (a) SSHA and (b) Bigeye tuna HR anomalies due to the dominant cycles for the annual and interannual band in EIO region.

Cross-correlation analyses between monthly SSHA and SOI were calculated for the period 1994 to 2005 (Fig. 6a). El Niño (negative SOI) has significant effects on variability of EIO SSHA, with strong correlation between the SOI and SSHA. This correlation is maximal when SOI leads SSHA by 5 months (Fig. 6a). During neutral El Niño conditions, the IOD positive phase is significantly anticorrelated with EIO SSHA at lag of ± 5 months (Fig. 6b). Moreover, the anticorrelation between SSHA and Bigeye tuna HR is modest but significant at lag of ± 2 months, with a negative SSHA corresponding to a significant HR (Fig. 6c). Therefore, during the negative phase of the SOI (such as during "El Niño" years), the SSHA is negative in the following months resulting in a growing number of hooks reaching the Bigeye tuna fishing layer and increasing the Bigeye tuna HR (Fig. 2c).
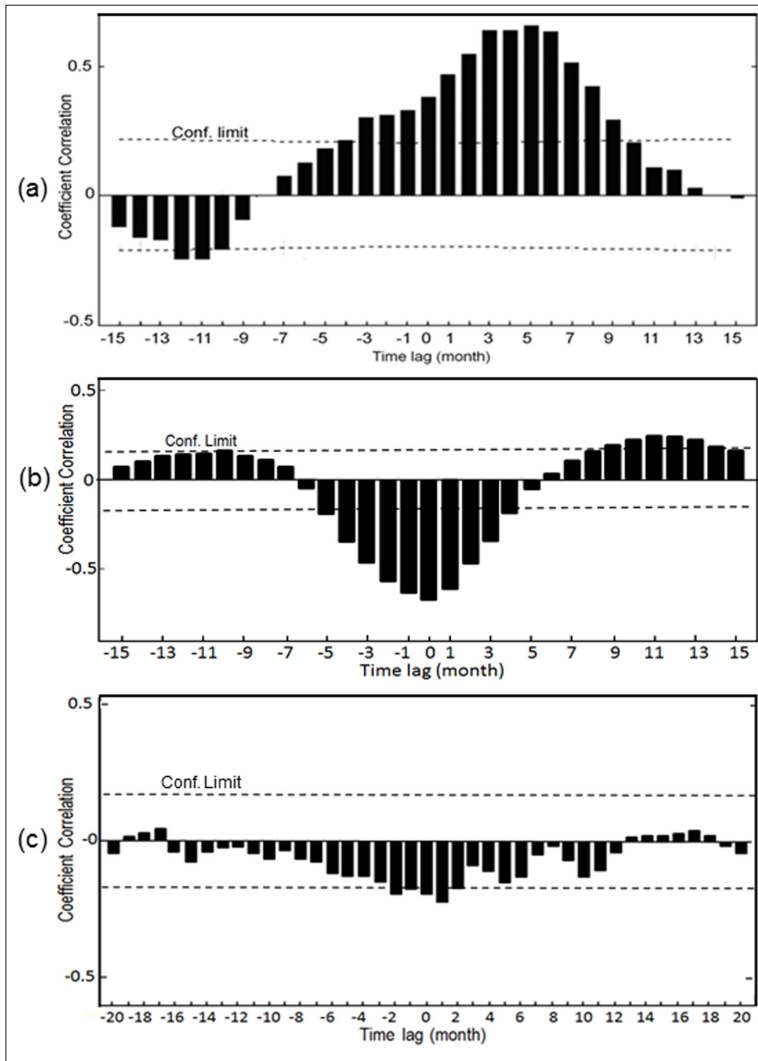
**Figure 6 - (a) Cross correlation coefficient between SOI and SSHA, (b) DMI and SSHA (c) SSHA and Bigeye tuna HR.**

SSHA and mechanism of fishing ground formation

During upwelling seasons and the El Niño and IOD positive event of 1997/98, large mesoscale eddies were observed in EIO. The highest Bigeye tuna HR (≥ 1.5) was found in the fronts between cyclonic and anti-cyclonic eddies (Fig. 7a). Frontal regions between eddies exhibit higher productivity and can be a feeding ground and also a barrier for tuna (Sund et al., 1981). This is similar to what is observed in North Atlantic where the Bigeye tuna HR was higher in region near mesoscale eddies than in non-eddy regions [Hsu, 2010]. Eddies create attractive pelagic habitats, analogous to oases in the desert, for higher trophic level aquatic organisms [Godø, 2012]. Mesoscale eddies typically form from baroclinic instability [Carton and Chao, 1999]. Eddy-induced upwelling exports nutrients from deep

water to the euphotic zone [McGillicuddy et al., 1997], and it is likely that this process contributes to eddy formation in the EIO region (Fig. 7b).

Mesoscale eddies affect the distribution of large predators in the marine ecosystem. Predators are attracted to different habitat that is influenced by eddy structure, polarities, and distribution [Hsu, 2010]. Mesoscale processes can enhance biological activity [Seki et al., 2000; Killwort et al., 2004], as has been seen by the higher Chl-a concentrations in cyclonic eddies observed in the EIO region (Fig. 7c). Normally, the highest Chl-a concentration in EIO region is found when upwelling process occurs during the southeast monsoon from June to October [Wyrtki, 1962; Susanto and Marra, 2005]; however, during El Niño and the 1997 IOD positive phase continuous blooming was observed through December in the EIO region (Fig. 7c), which may be one of causal factors increasing abundance of Bigeye tuna and catchability of longline fishing gear during those events.

Blooming of phytoplankton caused the abundance of oily sardine to increase in EIO region off Bali Strait [Lumban-Gaol, 2012]. Fishermen commonly used the oily sardine as bait for Bigeye tuna longline fishing, so extended abundance of oily sardine during El Niño/ IOD positive phase may coincide with the increase of Bigeye tuna abundance. Brill and Lutcavage [2001], concluded that Bigeye tuna tend to remain in the surface layer only at night and descend at dawn, behaviors that apparently allow them to exploit effectively the organisms of the deep scattering layer as prey.
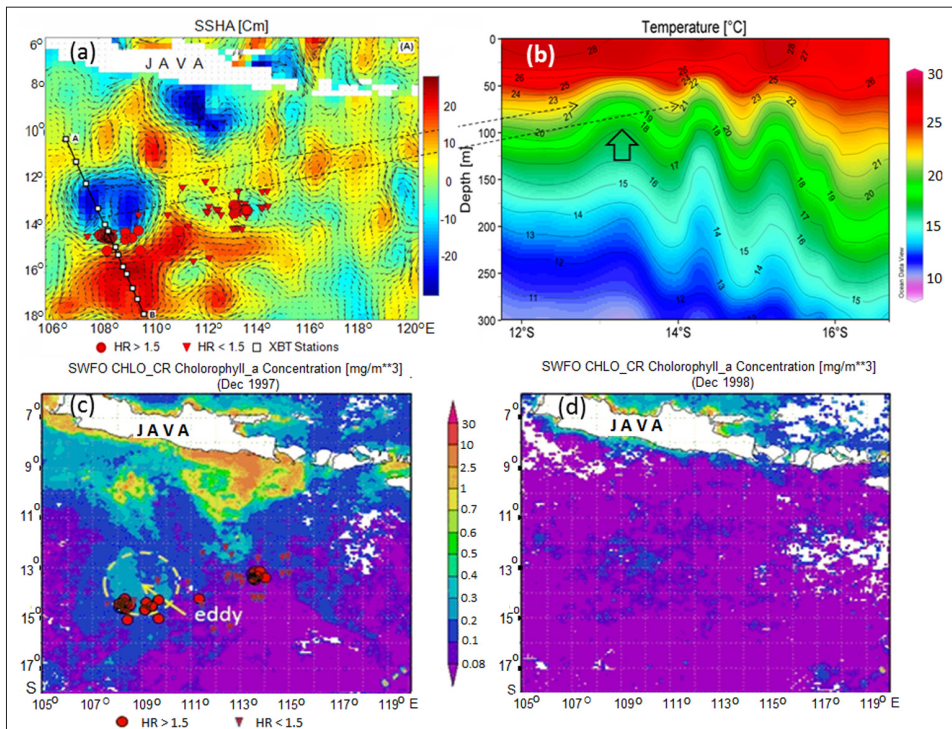
Figure 7 - (a) Bigeye tuna HR overlaid on SSHA, (b) Meridional section of temperature when eddy is well formed (c) Distribution of monthly mean Chl-a concentration at the time of El Niño and IOD positive phase in December 1997, (d) and normal condition in December 1998.

Conclusions

The variability of oceanographic parameters such as SST, SSHA, thermocline depth and Chl-a concentration in the EIO region were affected by monsoon season, El Niño and IOD events. During the southeast monsoon, upwelling occurs in the EIO region, characterized by colder SST, negative SSHA, shallowing thermocline depth, and increased Chl-a concentration of phytoplankton, and is more intense during El Niño and IOD positive phase. The negative correlation between SSHA and Bigeye tuna HR is modest but significant at lag of ± 2 months, with a negative (positive) SSHA corresponding to an increased (decreased) HR. The thermocline depth, which is shallower during the El Niño (negative SOI)/IOD positive phase events, is likely the causal factor contributing to higher than normal Bigeye tuna HR. The significant relationship between SSHA and thermocline depth, which is related to the Bigeye tuna fishing layer, indicates that SSHA is a useful indicator for identifying Bigeye tuna fishing grounds in EIO region.

Acknowledgement

References

Acker J.G., Leptoukh G. (2007) - *Online analysis enhances use of NASA earth science data*. Eos, Transactions American Geophysical Union, 88 (2): 14-17. doi: http://dx.doi.org/10.1029/ 2007EO020003/.

Amri K. (2012) - *Study of primary productivity on Indian Ocean dipole events and its relationship to pelagic fish catch abundance in western part of Sumatra waters*. Bogor Agricultural University Disertation, pp. 258.

Bray N.A., Hautala S., Chong J., Pariwono J. (1996) - *Large-scale sea level, thermocline, and wind variations in the Indonesian throughflow region.* Journal of Geophysical Research: Oceans (1978-2012), 101 (C5): 12239-12254. doi: http://dx.doi.org/ 10.1029/ 96JC00080/.

Brill R.W., Lutcavage M.E. (2001) - *Understanding environmental influences on movements and depth distributions of tunas and billfishes can significantly improve population assessments*. American Fisheries Society Symposium, 25: 179-198.

Carton J.A., Chao Y. (1999) - *Caribbean Sea eddies inferred from TOPEX/Poseidon altimetry and a 1/6 Atlantic Ocean model simulation*. Journal of Geophysical Research: Oceans (1978-2012), 104 (C4): 7743-7752. doi: http://dx.doi.org10.1029/ 1998 JC900081/.

Feng M., Meyers G. (2003) - *Interannual variability in the tropical Indian Ocean: a two-year time-scale of Indian Ocean Dipole*. Deep Sea Research Part II: Topical Studies in Oceanography, 50 (12): 2263-2284. doi: http:dx.doi.org/10.1016/S0967-0645(03)

00056-0.

Godfrey J.S. (1996) - *The effect of the Indonesian throughflow on ocean circulation and heat exchange with the atmosphere: A review*. Journal of Geophysical Research: Oceans (1978-2012), 101 (C5): 12217-12237. doi: http://dx.doi.org/10.1029/95JC03860.

Godø O.R., Samuelsen A., Macaulay G.J., Patel R., Hjøllo S.S., Horne, J., Kaartvedt J., Johannessen J.A. (2012) - *Mesoscale eddies are oases for higher trophic marine life.* PLoS ONE 7 (1): e30161. doi: http://dx.doi.org/10.1371/journal.pone.0030161.

Hanamoto E. (1987) - *Effect of oceanographic environment on Bigeye tuna distribution.* Bulletin of the Japanese Society of Fisheries Oceanography, 51 (3): 203-216.

Holland K.N., Brill R.W., Chang R.K.C. (1990) - *Movements of Thunnus albacares and Thunnus obesus near fish agregating devices*. Fish Bulletin-NOAA, 88: 494-507.

Hsu A.C.T. (2010) - *North Atlantic mesoscale eddy detection and marine species distribution*. Master Thesis, Duke University, Durham, 28 pp.

Killworth P.D., Cipollini C.P., Uz B.M., Blundell J.R. (2004) - *Physical and biological mechanism for planetary waves observed in satellite-derived chlorophyll*. Journal of Geophysical Research: Oceans (1978-2012), 109: 1029-1047. doi: http://dx.doi.org/10.1029/2003JC001768/.

Leben R.R., Born G.H., Engebreth B.R. (2002) - *Operational altimeter data processing for mesoscale monitoring.* Marine Geodesy, 25: 3-18.

Lehodey P., Bertignac M., Hampton J., Lewis A., Picaut J. (1997) - *El Niño Southern Oscillation and tuna in the western Pacific*. Nature 389 (6652): 715-718. doi: http://dx.doi.org/10.1038/39575.

Lumban-Gaol J., Mahapatra K., Okada Y. (2002) - *Tuna catch and ocean parameters derived satellite during ENSO 1997/98 in south Java Sea*. Fisheries Science, Supplement-I 68: 657-658. doi: http://dx.doi.org/10.2331/fishsci.68.sup1_657.

Lumban-Gaol J., Nababan B., Amri K., Hanggono A., Roswintiarti O. (2012) - *Climate change impact on Indonesian fisheries*. In: Griffiths J., Rowlands C., Witthaus M. (Eds.) Climate ExChage, pp. 73-74, Tudore Rose. England.

Lumban-Gaol J., Wudianto, Pasaribu B.P., Manurung D., and Arhatin R.E. (2004) - *The fluctuation of chlorophyll-a concentration derived from satellite imagery and catch of oily sardine (Sardinella lemuru) in Bali strait*. International Journal of Remote Sensing of Earth Science, 1 (1): 24-50.

Měnard F., Marsac F., Bellier E., Cazelles B. (2007) - *Climate oscillations and tuna catch in Indian Ocean: a wavelet approach to time series analysis.* Fisheries Oceanography, 16 (1): 95-104. doi: http://dx.doi.org/10.1111/j.1365-2419.2006. 00415.x.

Meyers G., McIntosh P., Pigot L., Pook M. (2007) - *The years of El Niño, La Niña, and interactions with the tropical Indian Ocean.* Journal of Climate, 20 (13): 2872-2880. doi: http://dx.doi.org/ 10.1175/JCLI4152.1.

Mohri M., Hanamoto E., Takeuchi S. (1996) - *Optimum water temperatures for Bigeye tuna [Thunnusobesus] in the Indian ocean as seen from tuna longline catches*. Bulletin of the Japanese Society of Scientific Fisheries (Japan), 62: 761-764.

McGillicuddy D.J., Robinson A.R. (1997) - *Eddy-induced nutrient supply and new production in the Sargasso Sea*. Deep Sea Research Part I: Oceanographic Research Papers, 44 (8): 1427-1450. doi: http://dx.doi.org/10.1016/S0967-0637(97)00024-1.

Rasmusson E.M., Carpenter T.H. (1982) - *Variations in tropical sea surface temperature*

and surface wind fields associated with the Southern Oscillation/El Niño. Monthly Weather Review, 110 (5): 354-384. doi: http://dx.doi.org/10.1175/1520-0493 (1982) 110<0354:VITSST> 2.0.CO;2.

Saji N.H., Goswami B.N., Vinayachandran P.N., Yamagata T. (1999) - *A dipole mode in the tropical Indian Ocean*. Nature, 401 (6751): 360-363. doi: http://dx.doi. org/10.1038/43854.

Saputra S.W., Solihin A., Wijayanto D., Kurohman F. (2011) - *Productivity and feasibility of tuna longliner on Cilacap district Central Java*. Saintek Perikanan, 6 (2): 78-84.

Seki M.P., Polovina J.J., Brainard R.E., Bidigare R.R., Leonard C.L., Foley, D.G. (2001) - *Biological enhancement at cyclonic eddies tracked with GOES thermal imagery in Hawaiian waters*. Geophysical Research Letters, 28 (8): 1583-1586. doi: http://dx.doi. org/10.1029/2000GL012439.

Susanto R.D., Gordon A.L., Zheng Q. (2001) - *Upwelling along the coasts of Java and Sumatra and its relation to ENSO*. Geophysical Research Letters, 28 (8): 1599-1602. doi: http://dx.doi.org/10.1029/2000GL011844/.

Susanto R.D., Marra J. (2005) - *Effect of the 1997/98 El Niño on chlorophyll-a variability along the southern coast of Java and Sumatra*. Oceanography, 18 (4): 124-127.

Susanto R.D., Moore T.S., Marra J. (2006) - *Ocean color variability in the Indonesian Seas during the SeaWiFS era*. Geochemistry, Geophysics, Geosystems, 7 (5): 1-16. doi: http://dx.doi.org/10.1029/2005GC001009.

Syamsudin M.L., Saitoh S.I., Hirawake T., Bachri S., Harto A.B. (2013) - *Effects of El Niño -Southern Oscillation events on catches of Bigeye tuna (Thunnus obesus) in the eastern Indian Ocean off Java*. Fishery Bulletin, 111 (2): 175-188. doi: http://dx.doi. org/10.7755/FB.111.2.5.

Sund P.N., Blackburn M., Williams F. (1981) - *Tunas and their environment in the Pacific Ocean: a review*. Oceanography marine biology annual review, 19: 443-512.

Torrence C., Compo G.P. (1998) - *A Practical Guide to Wavelet Analysis*. Bulletin of the American Meteorological Society, 79: 61 -78.

Tucker C.J., Yager K.A. (2011) - *Ten Years of MODIS in space: lessons learned and future perspectives*. Italian Journal of Remote Sensing, 43 (3): 7-18. doi: https://dx.doi.org/ 10.5721/ItJRS20114331.

Wyrtki K. (1962) - *The upwelling in the region between Java and Australia during the south-east monsoon*. Marine and Freshwater Research, 13 (3): 217-225. doi: http:// dx.doi.org/10.1071/MF9620217.

White W.B., Gloersen, K.A., Marsac, F., Tourre, Y.M. (2004) - *Influence of couple rossby waves on primary productivity and tuna abundance in the Indian Ocean*. Journal of Oceanography*, 60: 531-541. http://dx.doi.org/10.1023/b:joce.0000038346.28927.21.

Yu L. (2003) - *Variability of the depth of the 20 C isotherm along 6 N in the Bay of Bengal: Its response to remote and local forcing and its relation to satellite SSH variability*. Deep Sea Research Part II: Topical Studies in Oceanography, 50 (12): 2285-2304. doi: http://dx.doi.org/10.1016/S0967-0645(03)00057-2.